Reprinted from

Advances in Environmental Research

An international journal of research in environmental science, engineering and technology

OPTIMIZATION FRAMEWORK FOR MODELING THE LOW TEMPERATURE OXIDATION PROCESS FOR NOx REDUCTION

YAN FU[1], URMILA M. DIWEKAR[1,*] AND NARESH J. SUCHAK[2]

[1]*The Environmental Institute*
Carnegie Mellon University, Pittsburgh, PA 15213

[2]*BOC Gases, 575 Mountain Ave., Murray Hill, NJ 07974*

Advances in Environmental Research, **3** (4) 2000, 424-438

PERGAMON
An imprint of Elsevier Science

Pergamon

OPTIMIZATION FRAMEWORK FOR MODELING THE LOW TEMPERATURE OXIDATION PROCESS FOR NOx REDUCTION

YAN FU[1], URMILA M. DIWEKAR[1,*] AND NARESH J. SUCHAK[2]

[1]*The Environmental Institute*
Carnegie Mellon University, Pittsburgh, PA 15213

[2]*BOC Gases, 575 Mountain Ave., Murray Hill, NJ 07974*

Due to stringent environmental regulations, many industries will have to reduce their high levels of NOx emissions. A new process called Low Temperature Oxidation (LTO)** can reduce NOx emissions below measurable levels using process analyzers, and has been shown to be an attractive process to meet the stricter NOx regulations. However, the technology is relatively new and there is a strong need for research to identify the best way of configuring the process and finding an optimal design.

This paper presents a rigorous performance model for the LTO system for NOx removal based on a non-equilibrium modeling technique. A non-linear programming (NLP) optimization framework is employed to obtain the solution of the two-point boundary value problem. The basic framework proposed in this paper and the results of the studies will be used in the future for developing an efficient multi-objective optimization framework.

Key words: NOx reduction, NOx control, NOx removal, non-equilibrium modeling technique, non-linear programming, multi-objective optimization problem

INTRODUCTION

Nitrogen oxides (NOx) are a group of poisonous, brownish, highly reactive gases that form from fossil fuel combustion. NOx plays a major role, together with volatile organic compounds (VOCs), in the atmospheric reactions that contribute to ground-level ozone formation and acid rain, both of which have serious health and ecological effects [1]. Major human health effects include: lower resistance to respiratory illness and lung damage, and health hazards for infants. Major ecological effects include eutrophication, loss of visibility, acid rain, and dry acid deposition.

The two major NOx emissions sources are transportation and stationary fuel combustion, such as electric utility and industrial boilers. With the increasing emphasis on environmental concerns and the additional economic incentives of deregulation, many industries need tools to achieve low cost NOx removal.

There are currently two major categories of NOx control for stationary fuel combustion: combustion controls (e.g. low NOx burners, overfire air), and post-combustion controls (e.g. selective catalytic reduction or SCR, selective non-catalytic reduction or SNCR, and reburning) [2]. Combustion controls prevent the formation of NOx by delaying the mixing of fuel and air in the main combustion zone. Post-combustion controls destroy NOx that has formed in the main combustion zone by injecting ammonia (SCR), urea (SNCR), or additional fuel (reburning).

Current available combustion controls can, on average, reduce NOx by approximately 50 percent from uncontrolled levels. Post-combustion controls can either be applied in conjunction with combustion controls or by themselves. Depending upon how such controls are designed and engineered, they can reduce NOx as little as 30% or as much as 95% [2].

While NOx emissions can be reduced by changing combustion control, this often has a detrimental effect on its efficiency. In traditional SCR technology,

*Corresponding author. Fax: 412-268-3757; Email: urmila@cmu.edu

a catalyst must be employed in order to achieve significant NOx removal (in the temperature range of 450-1100 °F). However, the SCR process is expensive, and requires handling of two byproducts: (a) residual ammonia, due to imperfect mixing or reaction of the reagent; and (b) SO_3, which is oxidized from SO_2 by the catalyst. In the SNCR process, urea (NH_2COH_2) is typically injected into the flue gas near the furnace exit or in the convection pass to chemically reduce NOx to nitrogen (in the temperature range of 1700-2400 °F). The relatively high temperatures of the flue gas promote high reaction rates so a catalyst is not required for significant NOx removal. However, employing a urea reagent may produce N_2O (a "greenhouse" gas) as a byproduct. The SO_3 content of fuel gas is also a factor influencing SNCR feasibility when firing higher sulfur fuel oils and coals due to the potential for fouling some types of air heaters. Fuel reburning redistributes a portion of both fuel and air into the upper regions of the furnace to create a second flame zone, generating chemical reducing conditions to destroy NOx. Key factors influencing the technical feasibility of reburning are: whether sufficient residence time is available, the furnace corrosion resistance, and the cost of fuel.

In addition, the more stringent environmental rules, announced by the U.S. EPA on September 24, 1998, require 22 eastern states plus the District of Columbia to develop state implementation plans to reduce ground-level ozone through the reduction of NOx emissions [3]. This plan calls for a 28% NOx cut in the summer time (1.2 million tons) by 2007. Therefore, the development of new, efficient, and robust post-combustion NOx control technologies is even more necessary, important and urgent.

The LTO process, which can reduce NOx emissions below detection limits (2ppm) at low temperature (125-325 °F), was awarded the best available control technology (BACT) and the lowest available emission reduction technology (LAER) by EPA in April 1998. Ozone is employed to oxidize nitric oxide (NO) to dinitrogen pentoxide (N_2O_5) at low temperature in an oxidizer; it is then easily absorbed by water in a scrubber. Bench scale and pilot plant tests have shown that the LTO process can reduce the NOx emissions below the measurable levels using process analyzers (almost complete removal) (Cannon Technology, unpublished results). This proved that the LTO system is an attractive process to meet the stricter NOx regulations. There are multiple benefits of the LTO system in addition to removal of NOx emissions, including reduction of SOx and CO emissions, and no secondary air emissions (NH_3, N_2O). In order to obtain minimum NOx emissions, extra ozone needs to be supplied. The cost of the process also increases nonlinearly as emissions decrease. This poses a challenging multiobjective optimization problem where emissions like NOx and SOx need to be minimized, while minimizing the system cost as well as the use of extra ozone.

Optimization has been described as a three-step decision-making process [4]. The first step is attaining knowledge of the system and hence it is related to modeling the process. The second step involves finding a measure of system effectiveness. The third step is related to the theory of optimization, which involves application of a proper optimization algorithm to find a solution.

This paper presents the first step, a non-equilibrium model for the LTO system, towards an efficient multi-objective optimization framework for the LTO process. The complex chemistry associated with the process results in a two-point boundary value problem. An approach based on a non-linear programming optimization technique is used. This paper is divided into five sections. Section 2 describes the salient features of the LTO process. In Section 3, the chemistry of the non-equilibrium model is discussed. Section 4 addresses the two-point boundary value problem and introduces the optimization framework. Section 5 gives the conclusion of the current work and outlines future work pertaining to the multi-objective framework.

THE LTO PROCESS

Figure 1 shows the LTO process diagram for the industrial boiler application [5]. In Figure 1, the exhaust gases from the boiler are cooled in a high temperature economizer giving up heat to preheat the boiler feed water. The gas is then cooled to its dew-point temperature in the condensing economizer and a portion of the water vapor in the gas is condensed. Ozone is injected into the gas as it leaves the condensing economizer and is thoroughly mixed with the gas in a static mixer. The NOx in the gas is oxidized in the oxidation chamber to dinitrogen pentoxide (N_2O_5), while partial CO is oxidized to CO_2. The dinitrogen pentoxide forms nitric acid vapor as it contacts the water vapor in the gas. Then nitric acid vapor is absorbed in the scrubber as dilute nitric acid, and is then neutralized by a sodium carbonate solution in the scrubber forming sodium nitrate. Accordingly, sodium bicarbonate, sodium nitrite, sodium sulfite, and sodium sulfate are produced. These dilute salts can be discharged to the sanitary sewer system for small scale industrial boilers. For large scale systems byproduct recovery can be an option.

MATHEMATICAL MODEL

The two important unit operations which affect the chemistry of the LTO process are the oxidizer and the scrubber. The following addresses the non-equilibrium model for both.

The Oxidizer

Since oxidation of nitric oxide is an important step in NOx absorption, a mathematical model for the oxidizer is developed for low concentration of NOx in the flue gas based on a non-equilibrium modeling technique. Earlier work [6-8] showed that a non-equilibrium model was much more accurate than an equilibrium model for NOx absorption.

Flue gas from combustion consists of NOx, SOx, CO, CO_2, N_2, O_2 and particulate matter. In addition, it may contain hydrocarbons and heavy metals.

Ozone is a strong oxidant. When ozone is introduced in the flue gas stream, it oxidizes NOx and partial CO to higher oxides. At a temperature exceeding 325 °F it decomposes rapidly.

Figure 2 shows the schematic model of the oxidizer. Cooled flue gas coming from the outlet of the heat exchanger is thoroughly mixed with ozone and oxygen, generated from the ozone generator, at the inlet of the oxidizer duct. Multiple oxidation-reduction reactions take place along the length of the oxidizer duct. The oxidizer output contains the high oxides NOx, and other SOx and COx gases, which enter the bottom of the scrubber. Gases are removed in the scrubber by the dilute sodium carbonate solution.

Gas Phase Reactions

For the purpose of gas-phase reactor design, the following reactions are considered in modeling the oxidizer.

$$NO + O_3 \xrightarrow{k1} NO_2 + O_2 \quad (1)$$

$$2NO_2 + O_3 \xrightarrow{k2} N_2O_5 + O_2 \quad (2)$$

$$O_3 \xrightarrow{k3} 1.5O_2 \quad (3)$$

$$SO_2 + O_3 \xrightarrow{k4} SO_3 + O_2 \quad (4)$$

$$CO + O_3 \xrightarrow{k5} CO_2 + O_2 \quad (5)$$

$$NO + 0.5O_2 \xrightarrow{K6} NO_2 \quad (6)$$

$$N_2O_5 + H_2O \xrightarrow{K7} 2HNO_3 \quad (7)$$

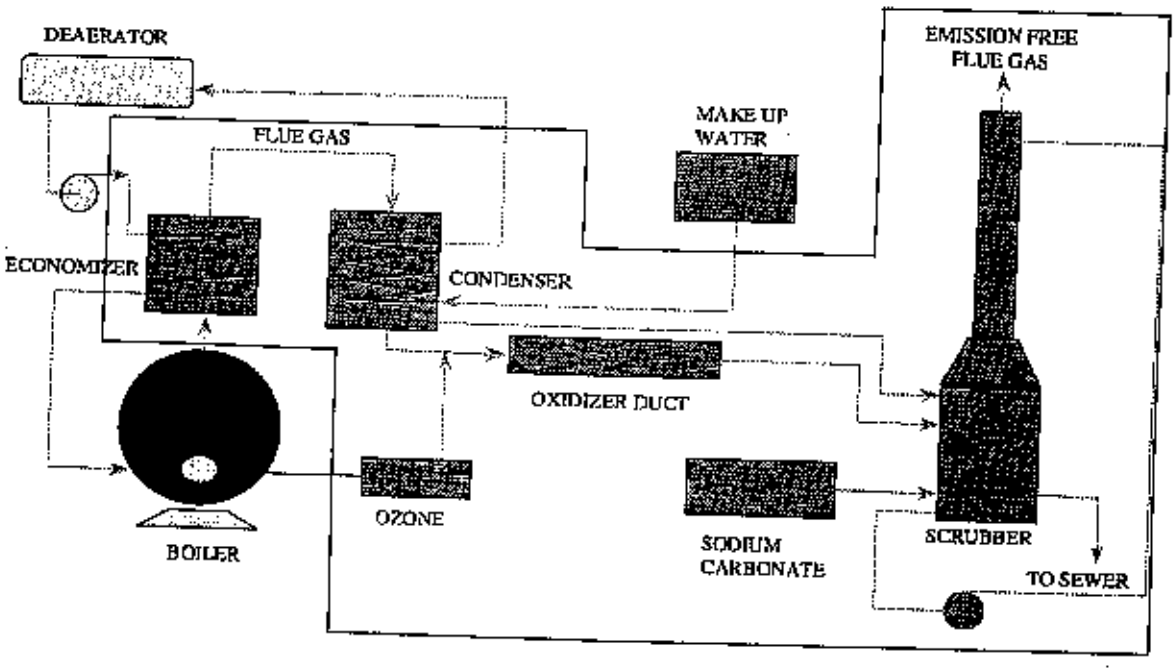

Figure 1. Low Temperature Oxidation (LTO) process diagram for industrial boiler applications.

$$SO_2 + N_2O_5 \xrightarrow{K8} SO_3 + 2NO_2 \quad (8)$$

Chemical reaction rates for these reactions are summarized as:

$$R_1 = k_1 P_{NO} P_{O_3} \quad (9)$$

$$R_2 = k_2 P_{NO_2} P_{O_3} \quad (10)$$

$$R_3 = 2k_3 P_{O_3}{}^2 / P_{O_2} \quad (11)$$

$$R_4 = k_4 P_{SO_2} P_{O_3} \quad (12)$$

$$R_5 = k_5 P_{CO} P_{O_3} \quad (13)$$

$$R_6 = k_6 P_{NO}{}^2 P_{O_2} \quad (14)$$

$$R_7 = k_7 P_{N_2O_5} P_{H_2O} \quad (15)$$

$$R_8 = k_8 P_{SO_2} P_{N_2O_5} \quad (16)$$

Mass Balance Over the Oxidizer

Considering the differential volume of the gas phase reactor, the following assumptions are made:

(1) Ozone and flue gas are thoroughly mixed (using static mixers ensures more than 99% mixing).
(2) Gases move in a plug flow manner.
(3) Gases follow ideal gas behavior.
(4) There are no radial gradients in temperature, concentration and density of the gas.
(5) The reactor is operating at the steady state.

Mass balances across a differential length *dl* at length *l* are given as:

(a) Divalent nitrogen oxide:

$$\frac{dY_{NO}}{dl} = -\frac{S}{G}\{R_1 + R_6\} \quad (17)$$

(b) Tetravalent nitrogen oxides:

$$\frac{dY_{NO_2}}{dl} = -\frac{S}{G}\{-R_1 + 2R_2 - R_6 - 2R_8\} \quad (18)$$

(c) Dinitrogen pentoxide:

$$\frac{dY_{N_2O_5}}{dl} = -\frac{S}{G}\{-R_2 + R_7 + R_8\} \quad (19)$$

(d) Nitrous acid: (Because of the large amount of ozone in the oxidizer, generating nitrous acid is a slow reaction compared to the other species. Therefore, we can assume the mass of nitrous acid does not change across a differential length in the oxidizer.)

$$\frac{dY_{HNO_2}}{dl} = 0 \quad (20)$$

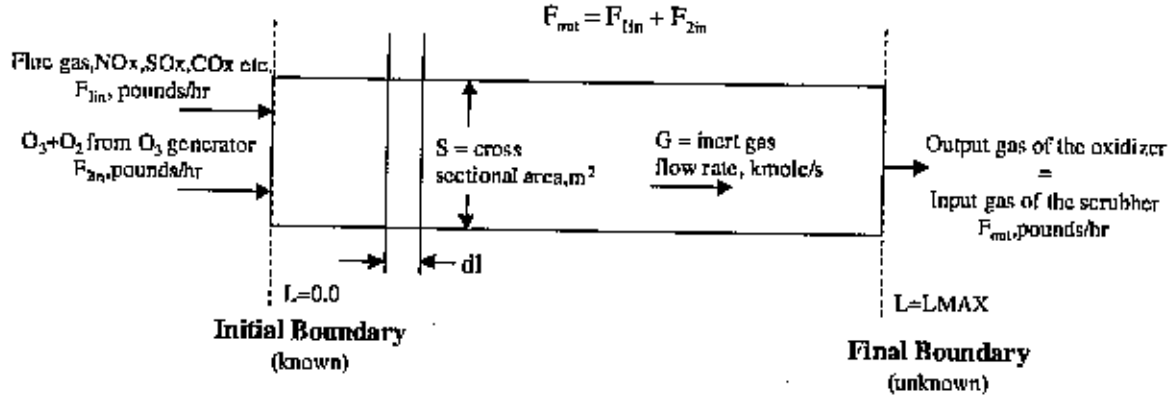

- **Non-equilibrium model**
- **Initial value problem**

Figure 2. Model for the oxidizer.

(e) Nitric acid:

$$\frac{dY_{HNO_3}}{dl} = -\frac{S}{G}\{-2R_7\} \quad (21)$$

(f) Sulfur dioxide:

$$\frac{dY_{SO_2}}{dl} = -\frac{S}{G}\{R_4 + R_8\} \quad (22)$$

(g) Sulfur trioxide:

$$\frac{dY_{SO_3}}{dl} = -\frac{S}{G}\{-R_4 - R_8\} \quad (23)$$

(h) Carbon monoxide:

$$\frac{dY_{CO}}{dl} = -\frac{S}{G}\{R_5\} \quad (24)$$

(i) Carbon dioxide:

$$\frac{dY_{CO_2}}{dl} = -\frac{S}{G}\{-R_5\} \quad (25)$$

(j) Oxygen:

$$\frac{dY_{O_2}}{dl} = -\frac{S}{G}\{-R_1 - R_2 - 1.5R_3 - R_4 - R_5 + 0.5R_6\} \quad (26)$$

(k) Ozone:

$$\frac{dY_{O_3}}{dl} = -\frac{S}{G}\{R_1 + R_2 + R_3 + R_4 + R_5\} \quad (27)$$

(l) Water vapor:

$$\frac{dY_{H_2O}}{dl} = -\frac{S}{G}\{R_7\} \quad (28)$$

(m) Nitrogen:

$$\frac{dY_{N_2}}{dl} = 0 \quad (29)$$

(n) Overall balance of total gases:

$$\frac{dY_T}{dl} = -\frac{S}{G}\{R_2 - 0.5R_3 + 0.5R_6 - R_8\} \quad (30)$$

Solution of differential equations

Equations 17–30 are coupled non-linear differential equations. The total mass balance is established across the differential element on solving these equations simultaneously. Mass balances for successive elements are obtained by integrating over the entire length of the reactor (in other words these equations are integrated for desired boundary conditions for given initial conditions of NOx conversions and ozone utilization). The mathematical model presented here is an initial value problem, as the input flow rate and composition of the gas are known. The equations are solved simultaneously by the fourth-order Runge-Kutta method based on earlier studies of the NOx absorber model [6]. The effect of step size for integration was examined and was selected in such a way that the result is independent of the step size. Integration is carried out until one (the first) of the stopping criteria is reached. The stopping criteria are listed as the following: (1) The NOx oxidation rate is greater than or equal to the desired NOx oxidation rate. (2) The total NOx outlet concentration is less than the desired operation need. (3) There is no more ozone left to further oxidize NOx to high oxides of nitrogen. (4) The maximum length of the oxidizer is reached.

Figure 3 shows the results of model simulations and experimental observations for the oxidizer model after fine tuning the model parameters. It is apparent that for different NOx/ozone mole ratios, the model predictions are in good agreement with experimental observations.

The Scrubber

Absorption of NOx gas is probably the most complex operation compared to other absorption processes. This is due to the following reasons:

(1) NOx gas is a mixture of several components, including N_2O, NO, NO_2, N_2O_3, N_2O_4 and N_2O_5. Absorption of NOx gas in water results in two oxyacids, nitric acid and nitrous acid.
(2) Several reversible and irreversible reactions occur in both gas and liquid phases.
(3) Simultaneous absorption of many gases occurs followed by chemical reaction. Heterogeneous equilibria prevail between gas and liquid phase components.
(4) For the process design of the scrubber, it is

necessary to understand the combined effects of several equilibria, the rates of mass transfer, and chemical reactions.

The situation in the scrubber is very complicated, in comparison to the oxidizer, because different mass transfer phenomena and chemical reactions take place simultaneously. Furthermore, the phenomena change in various parts of the scrubber [9]. Due to the complexity of the phenomena and its commercial interest, only a few advanced mathematical models [6-8, 10-11] have been published in the literature. However, most of these studies considered only NOx absorption, and focused on developing mathematical models for simulating the operation of the absorption tower in producing nitric acid. In the current scrubber tower, oxidation reactions continue in the gas phase, while simultaneous absorption of gases occurs at the gas-liquid interface. This is followed by multiple chemical reactions in the bulk liquid phase, where NOx, SOx, and COx are simultaneously absorbed by a dilute sodium carbonate solution, and $NaHCO_3$, Na_2CO_3, $NaNO_2$, $NaNO_3$, Na_2SO_3, Na_2SO_4 are formed in the liquid phase. This section presents an advanced mathematical model that is based on a steady-state mass balance using a non-equilibrium-modeling technique. The gas phase reactions, gas-phase mass transfer, liquid-phase mass transfer, and liquid phase reactions are included in the model.

Figure 4 shows the schematic model of the scrubber. The higher oxides NOx as well as other SOx and COx gases from the outlet of the oxidizer enter the bottom of the scrubber, while dilute sodium carbonate solution is sprayed from the top. Emission-free gases then leave the scrubber from the top and dilute salts solution exits from the bottom. The absorption is carried out in neural pH. This produces a countercurrent absorption process, with multiple chemicals, multiple mass transfers and multiple chemical reactions.

Gas phase reactions

The following reactions in the gas phase were considered in modeling the scrubber.

$$NO + O_3 \xrightarrow{k1} NO_2 + O_2 \quad (31)$$

$$2NO_2 + O_3 \xrightarrow{k2} N_2O_5 + O_2 \quad (32)$$

$$2O_3 \xrightarrow{k3} 3O_2 \quad (33)$$

$$SO_2 + O_3 \xrightarrow{k4} SO_3 + O_2 \quad (34)$$

$$CO + O_3 \xrightarrow{k5} CO_2 + O_2 \quad (35)$$

$$NO + 0.5O_2 \xrightarrow{K6} NO_2 \quad (36)$$

$$N_2O_5 + H_2O \xrightarrow{K7} 2HNO_3 \quad (37)$$

$$SO_2 + N_2O_5 \xrightarrow{K8} SO_3 + 2NO_2 \quad (38)$$

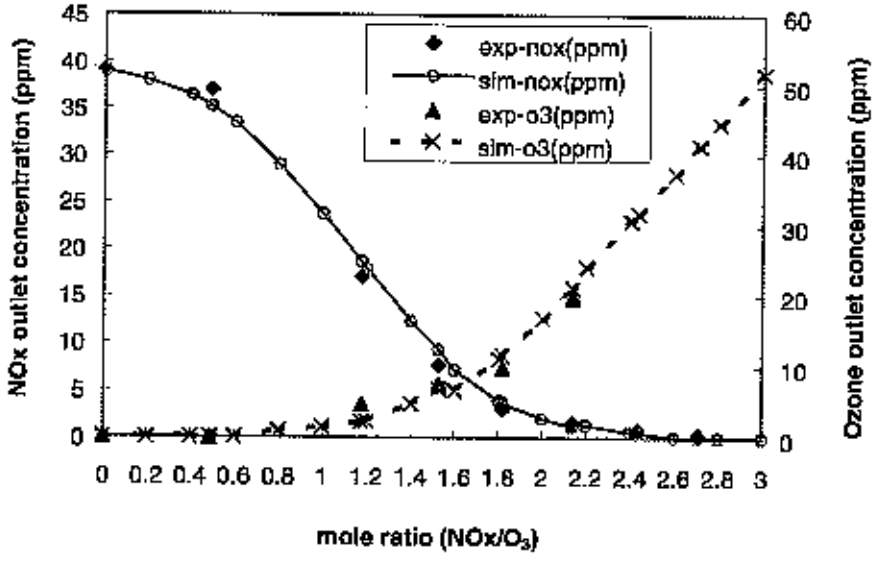

Figure 3. Comparison of model simulations and experimental observations for the oxidizer. (Experimental data courtesy of Cannon Technology.)

$$NO + NO_2 + H_2O \xrightarrow{K9} 2HNO_2 \quad (39)$$

Chemical reaction rates for these reactions are summarized as :

$$R_{G1} = k_1 P_{NO}{}^0 P_{O_3}{}^0 \varepsilon_G \quad (40)$$

$$R_{G2} = k_2 P_{NO_2}{}^0 P_{O_3}{}^0 \varepsilon_G \quad (41)$$

$$R_{G3} = 2k_3 (P_{O_3}{}^0)^2 / P_{O_2}{}^0 \varepsilon_G \quad (42)$$

$$R_{G4} = k_4 P_{SO_2}{}^0 P_{O_3}{}^0 \varepsilon_G \quad (43)$$

$$R_{G5} = k_5 P_{CO}{}^0 P_{O_3}{}^0 \varepsilon_G \quad (44)$$

$$R_{G6} = k_6 (P_{NO}{}^0)^2 P_{O_2}{}^0 \varepsilon_G \quad (45)$$

$$R_{G7} = k_7 P_{N_2O_5}{}^0 P_{H_2O}{}^0 \varepsilon_G \quad (46)$$

$$R_{G8} = k_8 P_{SO_2}{}^0 P_{N_2O_5}{}^0 \varepsilon_G \quad (47)$$

$$R_{G9} = 2k_9 P_{NO}{}^0 P_{NO_2}{}^0 P_{H_2O}{}^0 \varepsilon_G \quad (48)$$

Gas phase mass transfers

(a) Dinitrogen pentoxide:

$$N_2O_5(g) \xrightarrow{R21} N_2O_5(l) \quad (50)$$

$$R_{21} = R_{AN_2O_5,g} = \underline{a} k_{G,N_2O_5} (P^0_{N_2O_5} - P^i_{N_2O_5}) \quad (51)$$

(b) Nitric acid:

$$HNO_3(g) \xrightarrow{R22} HNO_3(l) \quad (52)$$

$$R_{22} = R_{AHNO_3,g} = \underline{a} k_{G,HNO_3} (P^0_{HNO_3} - P^i_{HNO_3}) \quad (53)$$

(c) Carbon dioxide:

$$CO_2(g) \xrightarrow{R23} CO_2(l) \quad (54)$$

$$R_{23} = R_{ACO_2,g} = \underline{a} k_{G,CO_2} (P^0_{CO_2} - P^i_{CO_2}) \quad (55)$$

(d) Sulfur trioxide:

$$SO_3(g) \xrightarrow{R24} SO_3(l) \quad (56)$$

$$R_{24} = R_{ASO_3,g} = \underline{a} k_{G,SO_3} (P^0_{SO_3} - P^i_{SO_3}) \quad (57)$$

(e) Sulfur dioxide:

$$SO_2(g) \xrightarrow{R25} SO_2(l) \quad (58)$$

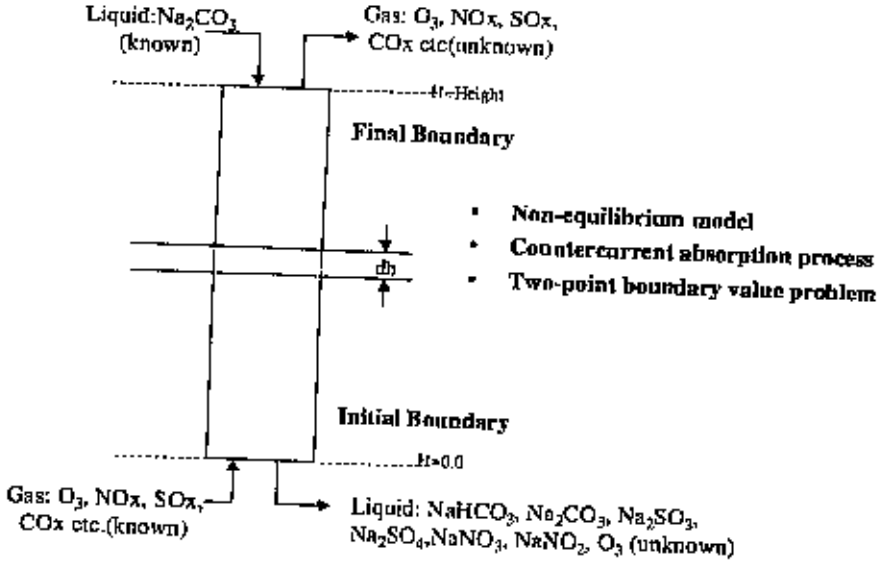

Figure 4. Model for the scrubber.

$$R_{25} = R_{A\mathrm{SO}_2,g} = \underline{a}k_{G,\mathrm{SO}_2}(P^0_{\mathrm{SO}_2} - P^i_{\mathrm{SO}_2}) \quad (59)$$

(f) Ozone:

$$\mathrm{O_3}(g) \xrightarrow{R26} \mathrm{O_3}(l) \quad (60)$$

$$R_{26} = R_{A\mathrm{O}_3,g} = \underline{a}k_{G,\mathrm{O}_3}(P^0_{\mathrm{O}_3} - P^i_{\mathrm{O}_3}) \quad (61)$$

(g) Nitrous acid:

$$\mathrm{HNO_2}(g) \xrightarrow{R27} \mathrm{HNO_2}(l) \quad (62)$$

$$R_{27} = R_{A\mathrm{HNO}_2,g} = \underline{a}k_{G,\mathrm{HNO}_2}(P^0_{\mathrm{HNO}_2} - P^i_{\mathrm{HNO}_2}) \quad (63)$$

(h) Water vapor:

$$\mathrm{H_2O}(g) \xrightarrow{R28} \mathrm{H_2O}(l) \quad (64)$$

$$R_{28} = R_{A\mathrm{H}_2\mathrm{O},g} = \underline{a}k_{G,\mathrm{H}_2\mathrm{O}}(P^0_{\mathrm{H}_2\mathrm{O}} - P^i_{\mathrm{H}_2\mathrm{O}}) \quad (65)$$

Liquid phase mass transfers

(a) Dinitrogen pentoxide absorption in water:

$$\mathrm{N_2O_5}(l) + \mathrm{H_2O}(l) \xrightarrow{R31} 2\mathrm{HNO_3}(l) \quad (66)$$

$$R_{31} = R_{A\mathrm{N}_2\mathrm{O}_5,l} = \underline{a}H_{\mathrm{N}_2\mathrm{O}_5}k_{LR,\mathrm{N}_2\mathrm{O}_5}P^i_{\mathrm{N}_2\mathrm{O}_5} \quad (67)$$

(b) Nitric acid absorption:

$$\mathrm{HNO_3}(l) \xrightarrow{R32} \mathrm{HNO_3}(l) \quad (68)$$

$$R_{32} = R_{A\mathrm{HNO}_3,l} = \underline{a}H_{\mathrm{HNO}_3}k_{L,\mathrm{HNO}_3}P^i_{\mathrm{HNO}_3} \quad (69)$$

(c) Carbon dioxide absorption:

$$\mathrm{CO_2}(l) \xrightarrow{R33} \mathrm{CO_2}(l) \quad (70)$$

$$R_{33} = R_{A\mathrm{CO}_2,l} = \underline{a}H_{\mathrm{CO}_2}k_{L,\mathrm{CO}_2}P^i_{\mathrm{CO}_2} \quad (71)$$

(d) Sulfur trioxide transfer:

$$\mathrm{SO_3}(l) \xrightarrow{R34} \mathrm{SO_3}(l) \quad (72)$$

$$R_{35} = R_{A\mathrm{SO}_3,l} = \underline{a}H_{\mathrm{SO}_3}k_{LR,\mathrm{SO}_3}P^i_{\mathrm{SO}_3} \quad (73)$$

(e) Sulfur dioxide transfer:

$$\mathrm{SO_2}(l) \xrightarrow{R35} \mathrm{SO_2}(l) \quad (74)$$

$$R_{36} = R_{A\mathrm{SO}_2,l} = \underline{a}H_{\mathrm{SO}_2}k_{LR,\mathrm{SO}_2}P^i_{\mathrm{SO}_2} \quad (75)$$

(f) Ozone transfer:

$$\mathrm{O_3}(l) \xrightarrow{R36} \mathrm{O_3}(l) \quad (76)$$

$$R_{36} = R_{A\mathrm{O}_3,l} = \underline{a}H_{\mathrm{O}_3}k_{LR,\mathrm{O}_3}P^i_{\mathrm{O}_3} \quad (77)$$

(g) Nitrous acid transfer:

$$\mathrm{HNO_2}(l) \xrightarrow{R37} \mathrm{HNO_2}(l) \quad (78)$$

$$R_{37} = R_{A\mathrm{HNO}_2,l} = \underline{a}H_{\mathrm{HNO}_2}k_{L,\mathrm{HNO}_2}P^i_{\mathrm{HNO}_2} \quad (79)$$

Liquid phase reactions

The following reactions in the liquid phase are considered in modeling the scrubber. Since there is no mass accumulated in the gas-liquid film, the gas phase mass transfer rate is equal to the liquid phase mass transfer rate for the same component. Further, the rates of reactions in the bulk liquid are so fast that they depend on the rates of mass transfers.

$$\mathrm{N_2O_5}(l) + \mathrm{Na_2CO_3}(l) \xrightarrow{R31} 2\mathrm{NaNO_3}(l) + \mathrm{CO_2}(g) \quad (80)$$

$$2\mathrm{HNO_3}(l) + \mathrm{Na_2CO_3}(l) \xrightarrow{R32} 2\mathrm{NaNO_3}(l) + \mathrm{CO_2}(l) + \mathrm{H_2O}(l) \quad (81)$$

$$\mathrm{CO_2}(l) + \mathrm{H_2O}(l) + \mathrm{Na_2CO_3}(l) \xrightarrow{R33} 2\mathrm{NaHCO_3}(l) \quad (82)$$

$$\mathrm{SO_3}(l) + \mathrm{Na_2CO_3}(l) \xrightarrow{R34} \mathrm{Na_2SO_3}(l) + \mathrm{CO_2}(g) \quad (83)$$

$$\mathrm{SO_2}(l) + \mathrm{Na_2CO_3}(l) \xrightarrow{R35} \mathrm{Na_2SO_3}(l) + \mathrm{CO_2}(g) \quad (84)$$

$$O_3(l) + Na_2SO_3(l) \xrightarrow{R36} Na_2SO_4(l) + O_2(g) \quad (85)$$

$$2HNO_2(l) + Na_2CO_3(l) \xrightarrow{R37} 2NaNO_2(l) + CO_2(g) + H_2O(l) \quad (86)$$

$$H_2O(l) \xleftrightarrow{R28} H_2O(g) \quad (87)$$

Mass balance over the scrubber

For the process design of the absorption tower, it is necessary to understand the combined effects of chemical reactions and mass transfer rates. The following are the mass balance equations in the gas phase across a differential height dh at height h from the bottom ($h = 0.0$):

Gas phase mass balances:

(a) Nitric oxide:

$$\frac{dY_{NO}}{dh} = -\frac{Sc}{G}\{R_{G1} + R_{G6} + R_{G9}\} \quad (88)$$

(b) Tetravalent nitrogen oxides:

$$\frac{dY_{NO_2}}{dh} = -\frac{Sc}{G}\{-R_{G1} + 2R_{G2} - R_{G6} - 2R_{G8} + R_{G9}\} \quad (89)$$

(c) Dinitrogen pentoxides:

$$\frac{dY_{N_2O_5}}{dh} = -\frac{Sc}{G}\{-R_{G2} + R_{G7} + R_{G8} + R_{21}\} \quad (90)$$

(d) Nitrous acid:

$$\frac{dY_{HNO_2}}{dh} = -\frac{Sc}{G}\{-2R_{G9} + R_{27}\} \quad (91)$$

(e) Nitric acid:

$$\frac{dY_{HNO_3}}{dh} = -\frac{Sc}{G}\{-2R_{G7} + R_{22}\} \quad (92)$$

(f) Sulfur dioxide:

$$\frac{dY_{SO_2}}{dh} = -\frac{Sc}{G}\{R_{G4} + R_{G8} + R_{25}\} \quad (93)$$

(g) Sulfur trioxide:

$$\frac{dY_{SO_3}}{dh} = -\frac{Sc}{G}\{-R_{G4} - R_{G8} + R_{24}\} \quad (94)$$

(h) Carbon monoxide:

$$\frac{dY_{CO}}{dh} = -\frac{Sc}{G}\{R_{G5}\} \quad (95)$$

(i) Carbon dioxide:

$$\frac{dY_{CO_2}}{dh} = -\frac{Sc}{G}\{-R_{G5}+R_{23}-R_{21}-0.5R_{22}-R_{24}-R_{25}-0.5R_{27}\} \quad (96)$$

(j) Oxygen:

$$\frac{dY_{O_2}}{dh} = -\frac{Sc}{G}\{-R_{G1}-R_{G2}-1.5R_{G3}-R_{G4}-R_{G5}+0.5R_{G6}-R_{36}\} \quad (97)$$

(k) Ozone:

$$\frac{dY_{O_3}}{dh} = -\frac{Sc}{G}\{R_{G1}+R_{G2}+R_{G3}+R_{G4}+R_{G5}+R_{26}\} \quad (98)$$

(l) Water vapor:

$$\frac{dY_{H_2O}}{dh} = -\frac{Sc}{G}\{R_{G7} + R_{G9} + R_{28}\} \quad (99)$$

(m) Nitrogen:

$$\frac{dY_{N_2}}{dh} = 0 \quad (100)$$

(n) Overall balance of total gases:

$$\frac{dY_T}{dh} = -\frac{Sc}{G}\{R_{G2} - 0.5R_{G3} + 0.5R_{G6} - R_{G8} + R_{G9} + R_{23} + R_{26} + R_{28} + 0.5R_{22} + 0.5R_{27}\} \quad (101)$$

Liquid phase mass balances:

(o) Sodium bicarbonate:

$$\frac{dX_{NaHCO_3}}{dh} = -\frac{Sc}{L}\{2R_{33}\} \quad (102)$$

(p) Sodium carbonate:

$$\frac{dX_{Na_2CO_3}}{dh} =$$

$$-\frac{Sc}{L}\{R_{31}+0.5R_{32}+R_{33}+R_{34}+R_{35}+0.5R_{37}\} \quad (103)$$

(q) Sodium sulfate:

$$\frac{dX_{Na_2SO_4}}{dh} = -\frac{Sc}{L}\{R_{34} + R_{36}\} \quad (104)$$

(r) Sodium sulfite:

$$\frac{dX_{Na_2SO_3}}{dh} = -\frac{Sc}{L}\{R_{35} - R_{36}\} \quad (105)$$

$$\frac{dX_{NaNO_2}}{dh} = -\frac{Sc}{L}\{R_{37}\} \quad (106)$$

(t) Sodium nitrate:

$$\frac{dX_{NaNO_3}}{dh} = -\frac{Sc}{L}\{R_{32} + 2R_{31}\} \quad (107)$$

(u) Ozone:

$$\frac{dX_{O_3}}{dh} = -\frac{Sc}{L}\{R_{36}\} \quad (108)$$

OPTIMIZATION FRAMEWORK FOR MODELING THE SCRUBBER

The mathematical model of the scrubber requires integrating twenty-one differential equations (88-108) along the height of the scrubber in order to get the gas and liquid phase concentrations at the top. The numerical integration technique requires the values of both liquid and gas phase components at $h = 0.0$ to start the integration. However, at $h = 0.0$, the liquid phase concentrations correspond to the outlet concentrations of the liquid, which are dictated by the chemical-absorption occurring in the column and are unknown. Here the condition is different from the nitric acid tower models presented in the literature where the outlet concentration was specified for nitric acid. Because multiple species are present in the liquid outlet of the LTO process, it is not possible to specify concentrations for all species. This results in a two-point boundary value problem, where the inlet concentrations of the gas phase at $h = 0.0$ and the inlet concentrations of the liquid phase at h = height (two boundaries) are known. The solution to this problem is iterative. Here we are using a systematic nonlinear programming (NLP) optimization procedure to solve this problem. Therefore, it can be easily said that the optimization technique is not only used for finding an optimal design but also for modeling.

$$\text{Obj. fun.} = \sum_{i=1}^{7}[X_i^P(h=H) - X_i^S(h=H)]^2 \quad (109)$$

where $X_i^P(h=H)$ is the predicted value of input liquid concentration for component i (mole of component i/mole of water), and $X_i^S(h=H)$ is the specified value of input liquid concentration for component i (mole of component i/mole of water).

$i = 1$ is $NaHCO_3$
$i = 2$ is Na_2CO_3
$i = 3$ is Na_2SO_4
$i = 4$ is Na_2SO_3
$i = 5$ is $NaNO_2$
$i = 6$ is $NaNO_3$
$i = 7$ is O_3

Figure 5 shows the optimization framework for finding the solution of the two-point boundary value problem in the scrubber. Initially, the values of the output liquid concentrations (decision variables) and given concentrations of the input gas phase are supplied to the model of the scrubber, which then calculates the concentrations at the other end. The liquid concentrations at $h = H$ represent the inlet concentrations of different components in the liquid phase, and are given. The objective function here is the sum of square errors of predicting concentrations of input liquid phase components as shown in Equation 109, which is minimized. If the predicted values of the inlet liquid do not match to the specified concentrations, the optimizer selects new values of outlet concentrations for the liquid phase according to the derivative directions based on the Sequence Quadratic Programming (SQP) method [12]. The iteration continues until the Kuhn-Tucker error that defines the optimality condition is approximately zero. This completes the modeling exercise.

Table 1 shows results of the optimization exercise used to solve the two-point boundary value problem. Heuristic values for output liquid concentrations at $h = 0.0$ are calculated according to Equations 110–116 below. The twenty-one differential equations (88–108) above are then integrated along the height of the scrubber to get the corresponding concentrations for the input liquid and the output gas at $h = H$. The fourth-order Runge-Kutta method is employed to solve the above equations simultaneously.

$$X^{H}_{NaHCO_3}(h=0) = X^{S}_{Na_2CO_3}(h=H) \tag{110}$$

$$X^{H}_{Na_2CO_3}(h=0) = X^{S}_{Na_2CO_3}(h=H) \tag{111}$$

$$X^{H}_{Na_2SO_4}(h=0) =$$

$$\frac{G}{L} * (0.1 * Y^{S}_{SO_2}(h=0) + Y^{S}_{SO_2}(h=0)) * 1.1 \tag{112}$$

$$X^{H}_{Na_2SO_3}(h=0) =$$

$$\frac{G}{L} * (Y^{S}_{SO_2}(h=0) + 0.1 * Y^{S}_{SO_2}(h=0)) * 1.1 \tag{113}$$

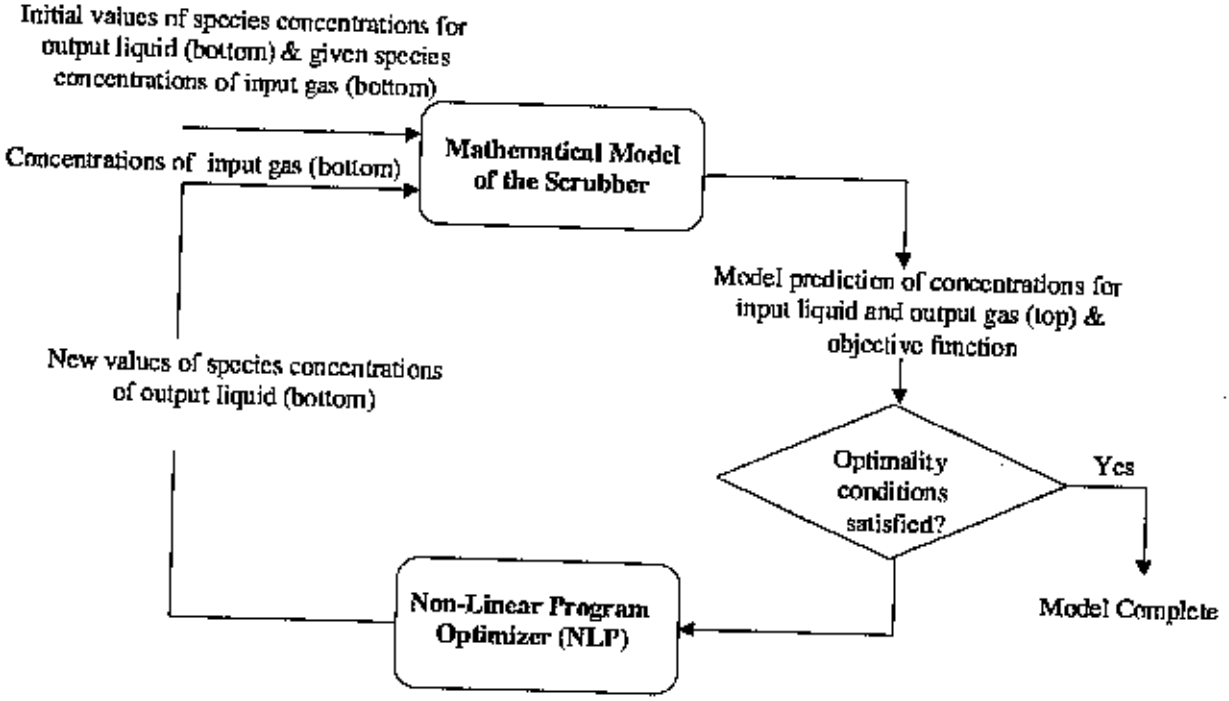

Figure 5. The optimization framework for solving the two-point boundary value problem.

$$X^{H}_{NaNO_2}(h=0) =$$

$$\frac{G}{L} * \{0.1 * [2 * Y^{S}_{N_2O_5}(h=0) + Y^{S}_{HNO_2}(h=0)] + Y^{S}_{HNO_3}(h=0) + Y^{S}_{NO}(h=0) + Y^{S}_{NO_2}(h=0)\} * 1.1 \quad (114)$$

$$X^{H}_{NaNO_3}(h=0) =$$

$$\frac{G}{L} * [2 * Y^{S}_{N_2O_5}(h=0) + Y^{H}_{HNO_2}(h=0) + 0.5 * [Y^{S}_{HNO_3}(h=0) + Y^{S}_{NO}(h=0) + Y^{S}_{NO_2}(h=0)]\} * 1.1 \quad (115)$$

$$X^{H}_{O_3}(h=0) = \frac{G}{L} * Y^{S}_{O_3}(h=0) * 1.1 \quad (116)$$

where $X^{H}_{x}(h=0)$ means the heuristic value of output liquid concentration for component x (mole of component x/mole of water), $X^{S}_{x}(h=H)$ means the specified value of input liquid concentration for component x (mole of component x/mole of water), $Y^{S}_{x}(h=0)$ means the specified value of input gas concentration for component x (mole of component x/mole of N_2), G means the gas phase flow rate of inert N_2 (kmoles of N_2/S), L means the liquid phase flow rate of inert H_2O (kmoles of H_2O /S), and H is the maximum height of the scrubber (m).

These heuristic values at $h = 0.0$ are used for the initial estimation of output liquid concentrations to integrate the above twenty-one equations (88-108) simultaneously along the height of the scrubber and obtain the corresponding input values for the liquid concentrations. The error in the prediction of input liquid concentrations is minimized using the NLP optimizer with the output liquid concentrations at $h = 0.0$ as the decision variables. Results in Table 1 prove that the optimizer is able to match the inlet liquid concentrations and these results are not sensitive to initial values of output liquid concentrations.

Figure 6 shows the objective function and the Kuhn-Tucker error versus the number of iterations. The objective is minimized at the end of twenty iterations, predicting input liquid concentrations closer to the specified values.

Figure 7 shows the results of model simulations and experimental observations for the complete LTO system (oxidizer + scrubber). Similar to the oxidizer results, the figure shows that the model and experiments match well (within 5% error).

CONCLUSION

This paper has modeled a new NOx reduction process. The process shows great promise for NOx reduction as well as removal of other emission

Table 1. Results of using the optimization framework to solve the two-point boundary value problem.

Components in the liquid phase	Specified concentrations of input liquid (top) *** x10^6	Heuristic values for concentrations of output liquid (bottom) *** x10^6	Corresponding values for concentrations of input liquid (top) *** x10^6	Predicted values for concentrations of output liquid (bottom) *** x10^6	Predicted values for concentrations of input liquid (top) *** x10^6
$NaHCO_3$	0.0000	1715.3	1713.7	1.4953	0.0000
Na_2CO_3	1700.0	1715.3	1851.7	1565.4	1701.8
Na_2SO_4	0.0000	4.6164	4.6157	1.8049	1.8043
Na_2SO_3	0.0000	45.267	4.1235	38.069	0.0000
$NaNO_2$	0.0000	47.611	47.611	4.2231	4.2231
$NaNO_3$	0.0000	193.30	4.3460	188.41	0.0000
O_3	0.0000	36.139	3.3653	19.550	0.0000

*** The above are dimensionless concentrations, mole of component/mole of water.

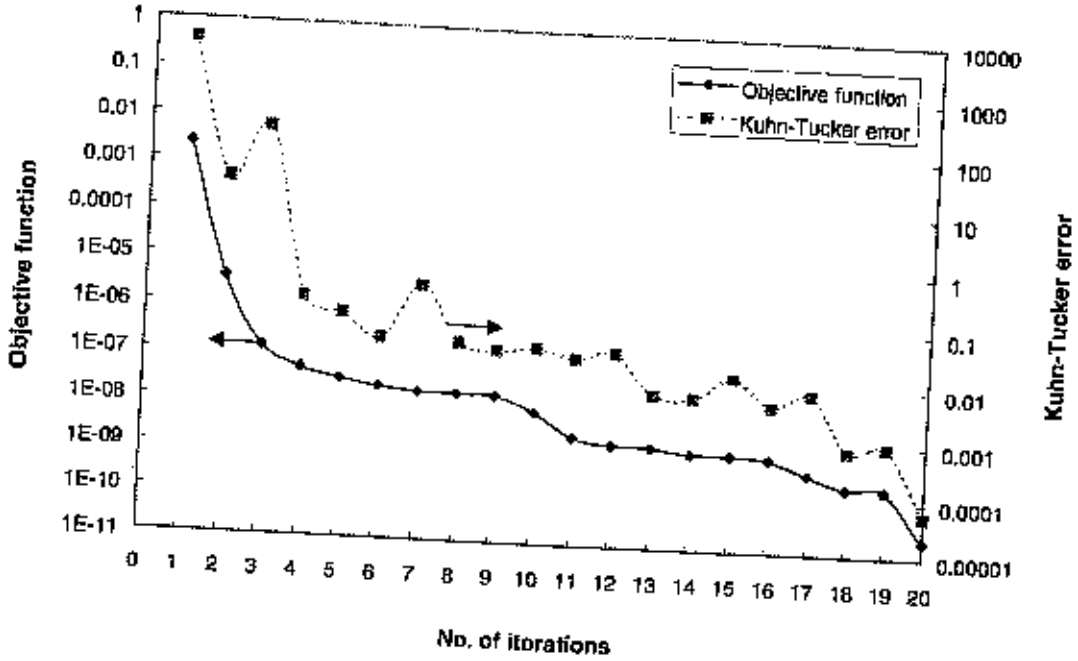

Figure 6. The objective function and the Kuhn-Tucker error versus the number of iterations.

products such as SOx and CO. Non-equilibrium models for the oxidizer and scrubber operation units are developed. The model simulations matched experimental results. This paper also identified a major difficulty in modeling these unit operations as a two-point boundary value problem. This two-point boundary value problem mainly associated with the NOx scrubber due to complex reactions involved with multiple species. This paper presented an optimization framework to solve this two-point boundary value problem iteratively.

In the future, the LTO process model will be

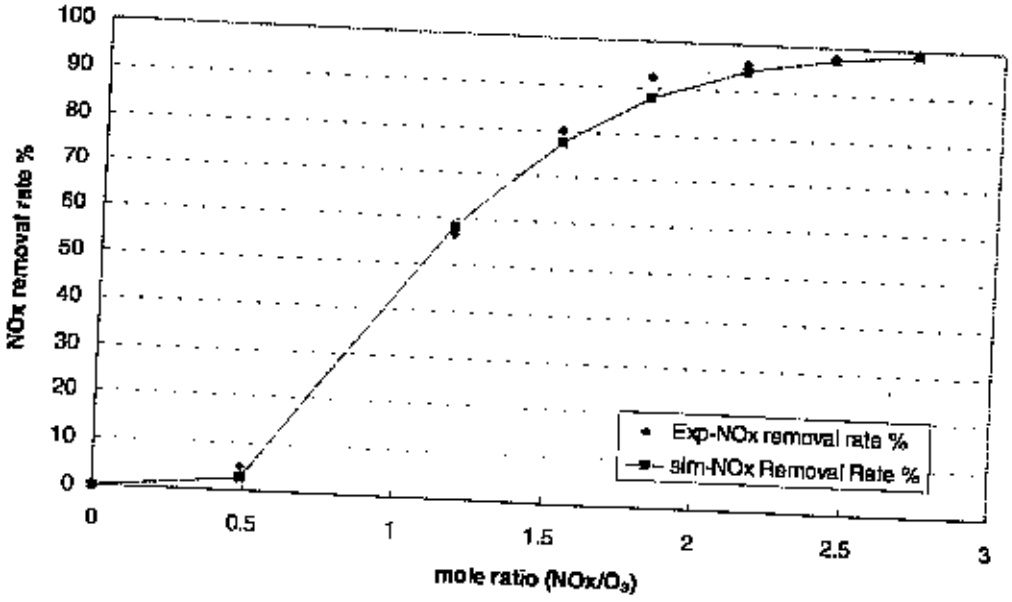

Figure 7. Comparison of model simulations and experimental observations for the combined LTO process. (Experimental data courtesy of Cannon Technology.)

used to solve the multi-objective problem to obtain minimum cost and emission designs. Figure 8 shows the strategy for this multi-objective optimization framework. The LTO non-equilibrium model will be augmented with the cost model of the process. It can be seen from Figure 8 that the objective function in the modeling exercise (error in the prediction of inlet liquid concentrations) is converted to a constraint. This will permit simultaneous solution of the modeling and the optimization problems. The objective surface for the multi-objective problem will be obtained. This surface will be helpful for redesigning the system to make it cost efficient while maintaining its advantage of very low levels of all kinds of pollutant emissions.

ACKNOWLEDGEMENTS

We acknowledge the financial support of the Pennsylvania Infrastructure Technology Alliance (PITA). Partial fund is provided by EPA's grant CR 826085-01-0, Cannon Technology Inc. and BOC Gases. The authors also want to thank Dr. Wesley M. Rohrer and Dr. John M. Koltick of Cannon Technology Inc. for useful discussions. Tim Johnson for technical editing.

NOMENCLATURE

a	interfacial area, m^2/m^3
D_x	diffusion coefficient of component x, m^2/s
G	flow rate of inert N_2 in the gas phase, kmoles of N_2/s
H	the maximum height of the scrubber, m
H_x	Henry's law coefficient of component x, (kmoles m^2)/(kN/m^2)
k_i	forward gas phase reaction rate constant for Equation i and Equation $3i$
k_9	forward gas phase reaction rate constant for Equation 39
$k_{G,x}$	gas-side mass transfer coefficient of component x, kmoles/(kN/m^2·s)
$k_{L,x}$	liquid-side mass transfer coefficient of component x, kmoles/(kN/m^2·s)
$k_{LR,x}$	mass transfer coefficient of component x with enhancement due to chemical reaction, kmoles/(kN/m^2·s)
L	flow rate of inert H_2O in the liquid phase, kmoles of H_2O /s
P_x	partial pressure of component x in the gas phase of the oxidizer, kN/m^2

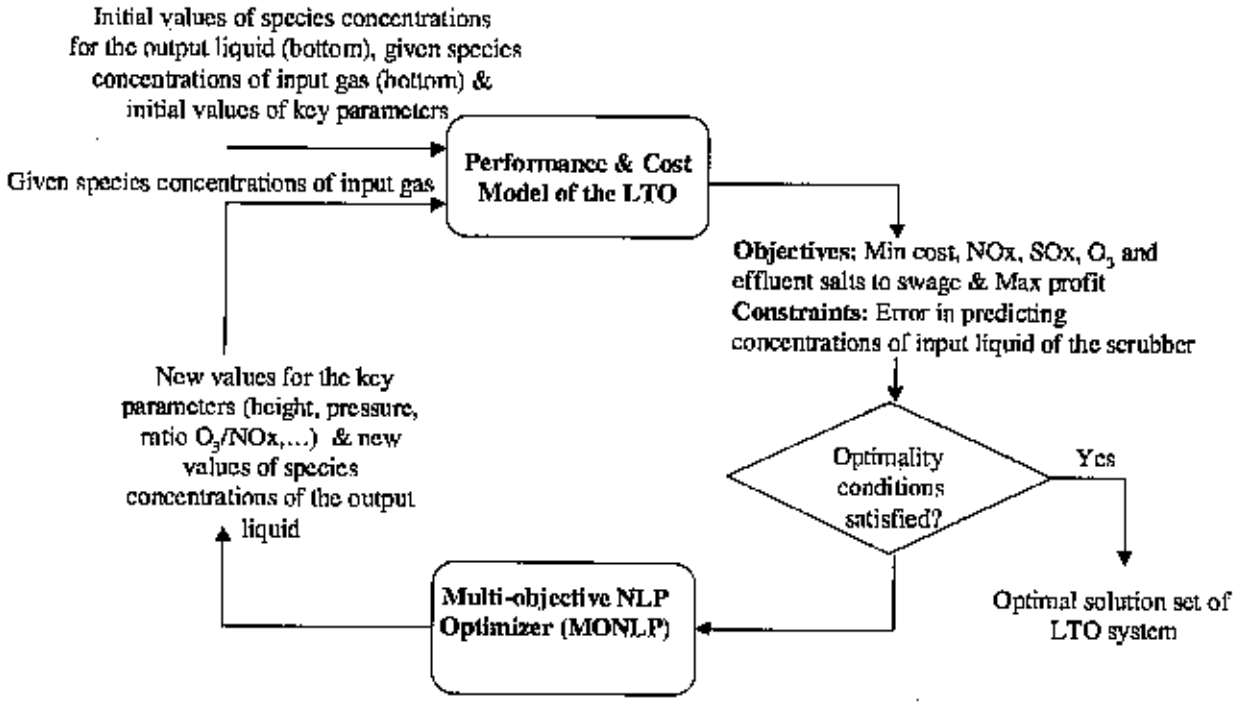

Figure 8. The multi-objective optimization framework for Low Temperature Oxidation (LTO) system.

P_x^0 partial pressure of component x in the bulk gas phase of the scrubber, kN/m^2

P_x^i partial pressure of component x at the gas-liquid interface of the scrubber, kN/m^2

R_i forward gas phase reaction rate of Equation i in the oxidizer, kmoles/(m^3.s)

R_{Gi} forward gas phase reaction rate of Equation $3i$ in the scrubber, kmoles/(m^3.s)

R_{21} rate of gas-side maSss transfer of N_2O_5, kmoles/(m^3.s)

R_{22} rate of gas-side mass transfer of HNO_3, kmoles/(m^3.s)

R_{23} rate of gas-side mass transfer of CO_2, kmoles/(m^3.s)

R_{24} rate of gas-side mass transfer of SO_3, kmoles/(m^3.s)

R_{25} rate of gas-side mass transfer of SO_2, kmoles/(m^3.s)

R_{26} rate of gas-side mass transfer of O_3, kmoles/(m^3.s)

R_{27} rate of gas-side mass transfer of HNO_2, kmoles/(m^3.s)

R_{28} rate of gas-side mass transfer of H_2O, kmoles/(m^3.s)

R_{31} rate of liquid-side mass transfer of N_2O_5, kmoles/(m^3.s)

R_{32} rate of liquid-side mass transfer of HNO_3, kmoles/(m^3.s)

R_{33} rate of liquid-side mass transfer of CO_2, kmoles/(m^3.s)

R_{34} rate of liquid-side mass transfer of SO_3, kmoles/(m^3.s)

R_{35} rate of liquid-side mass transfer of SO_2, kmoles/(m^3.s)

R_{36} rate of liquid-side mass transfer of O_3, kmoles/(m^3.s)

R_{37} rate of liquid-side mass transfer of HNO_2, kmoles/(m^3.s)

$R_{Ax,g}$ rate of gas-phase mass transfer of component x, kmoles/(m^3.s)

$R_{Ax,l}$ rate of absorption of component x, kmoles/(m^3.s)

S cross-section area of the oxidizer, m^2

S_C cross-section area of the scrubber, m^2

X_x kmoles of component x per kmoles of water, liquid phase

Y_x kmoles of component x per kmoles of inerts, gas phase

Y_T total kmoles of gases per kmoles of inerts, gas phase

ε_G fractional gas hold-up

REFERENCES

1. US EPA, (1996), National Air Quality and Emissions Trends Report, (EPA Document Number 454/R-97-013) Chapter 2, pp.17-20.
2. Colburn, K. (1996) States' Report on Electric Utility Nitrogen Oxides Reduction Technology Options for Application by the Ozone Transport Assessment Group — April 11, 1996 5A-1, the Ozone Transport Assessment Group (OTAG) Final Report.
3. Cooper, C. (1998) EPA Imposes 28% NOx Cut by 2007, *Chemical Engineering*, November: pp. 54.
4. Beighter, C. S., Phillips, D. T. and Wilde, D. J. (1967) Foundations of Optimization, Prentice-Hall Inc., Englewood Cliffs, N. J.
5. Anderson, M. H., Skelley, A. P., Goren, E. and Gavello, J. (1998) A low temperature oxidation system for the control of NOx emissions using ozone injection, *ICAC Annual Meeting, Forum '98 Cutting NOx Emissions*: pp. 1-12.
6. Suchak, N. J., Jethani, K. R. and Joshi, J. B. (1991) Modeling and simulation of NOx absorption in Pilot-Scale Packed Columns, *AIChE Journal*, **37**(3): pp. 323-339.
7. Suchak, N. J. and Joshi, J. B. (1994) Simulation and optimization of NOx absorption system in nitric acid manufacture, *AIChE Journal*, **40**(6): pp. 944-956.
8. Pradhan, M. P., Suchak, H. J., Walse, P. R. and Joshi, J. B. (1997) Multicomponent gas absorption with multiple reactions: modeling and simulation of NOx absorption in nitric acid manufacture, *Chemical Engineering Science*, **52**(24): pp. 1-23.
9. Graham, H. G., Lyons, V. E. and Faucett, H. L. (1964) Concentrated nitric acid, *Chem. Engng. Progr.* **60**: pp. 77-84.
10. Joshi, J. B., Mahajani, V. V. and Juvekar, V. A. (1985) Absorption of NOx gases, *Chem. Eng. Commun.* **33**: pp. 1-92.
11. Holma, H. and Sohlo, J. (1979) A mathematical model of a absorption tower of Nitrogen Oxides in nitric acid production, *Computer & Chemical Engineering*, **3**: pp. 135-141.
12. Diwekar U. M., Rubin, E. S. and Frey, H. C. (1997) Optimal design of advanced power systems under uncertainty, *Energy Conversion and Management Journal*, 38: pp. 1725-1732 .

** The Low Temperature Oxidation System is Cannon Technology's patent. It is being commercialized independently by Cannon Technology as the LTO™ System, and by BOC Gases as the LoTOx™ System.